

Observation of large magnetoresistance switching in topological-insulator/ferromagnetic-metal heterostructure with perpendicular magnetic anisotropy

Junseok Oh ¹, Vincent Humbert,² Gregory J. MacDougall ^{1,3}, Matthew J. Gilbert,⁴ and Nadya Mason¹

¹*Department of Physics, University of Illinois at Urbana-Champaign, Urbana, Illinois 61801, USA*

²*Unite Mixte de Physique, CNRS, Thales, Universite Paris-Saclay, 91767 Palaiseau, France*

³*Materials Research Laboratory, University of Illinois at Urbana-Champaign, Urbana, Illinois 61801, USA*

⁴*Department of Electrical and Computer Engineering, University of Illinois at Urbana-Champaign, Urbana, Illinois 61801, USA*



(Received 1 August 2023; accepted 26 March 2024; published 8 May 2024)

In the last decade, studies of magnetoresistance in heterostructures of topological insulator (TI) and ferromagnetic (FM) insulators have indicated the existence of induced magnetization at TI surfaces. However, the magnetic proximity effect in heterostructures of TIs and FM metals has been less explored. Here, we report a spin-valve-like magnetoresistance (MR) switching observed in a bilayer device of Bi_2Se_3 and a Co/Pt multilayer ([Co/Pt]), where the [Co/Pt] is a FM metal with a perpendicular magnetic anisotropy. This MR switching happens at temperatures below 1 K and for magnetic field sweeps along all in-plane and out-of-plane directions, at values much lower than the magnetization switching fields of the top FM layer. The in-plane field sweeps at various angles also reveal a threefold symmetry of the switching fields, matching the symmetry of the TI crystal structure. We suggest that the large MR switching rises from the interplay between the magnetization of the top FM metal layer and the induced magnetization at the TI surface.

DOI: [10.1103/PhysRevMaterials.8.054202](https://doi.org/10.1103/PhysRevMaterials.8.054202)

I. INTRODUCTION

The gapless Dirac surface states in three-dimensional (3D) topological insulators (TIs) are protected from backscattering by time-reversal symmetry and have spin orientation locked to momentum, a property called spin-momentum locking [1–4]. The surface state can be gapped by inducing magnetic moments normal to the surface, which breaks the time-reversal symmetry. Due to such highly-spin-dependent properties, TIs serve as a good platform to study exotic transport phenomena in the presence of magnetism, such as the quantum anomalous Hall effect in magnetically doped [5,6] or intrinsically magnetic TIs [7–9]. In terms of spintronic applications, the highly-spin-dependent transport in TI surfaces also helps efficient spin-orbit torque switching in TI/magnet bilayer structures, as has been demonstrated in various combinations of TIs and magnetic layers [10–15].

A common way to induce magnetism in nonmagnetic TIs is through chemical doping with elements such as Cr [5] or V [6]. However, chemically doping TIs could introduce spatial inhomogeneity of the magnetic dopants and surface gaps along with deformation of the original TI crystal structure [16,17]. This leads to the Curie temperature of such magnetically doped TIs being very low (< 1 K), not ideal for potential spintronic applications. An alternative way to magnetize the TI surface is via exchange coupling to an adjacent magnetic layer [18,19]. In contrast to magnetically doped TIs, bilayers of a TI and an insulating magnetic layer have shown magnetotransport [20–27] and/or neutron reflectivity [28] signals of magnetized TI surfaces persisting to relatively high temperatures, even above room temperature in some cases [22,28]. Magnetizing TI surfaces via proximity

coupling has thus become a popular approach to manipulating surface-state properties at higher temperatures.

On the other hand, the effects of proximity magnetization in TIs are underinvestigated in spintronics research that uses a TI as a spin-charge conversion layer. In particular, many current-induced magnetization switching experiments examine bilayers of a TI and a metallic FM [10,11,13–15], but the magnetic proximity effect is not often taken into account. It has been predicted that interface states with Rashba-like spin-momentum locking will occur despite the hybridization to the metallic FM [29]. Furthermore, a careful calculation showed Co/Pt multilayer, a metallic FM with perpendicular magnetization, can magnetize the surface of the bottom TI layer, leading to a gap in the system's energy spectrum [30]. It is thus important to experimentally demonstrate that TI states strongly coupled to a metallic FM will contribute significantly to the systems transport, especially at a low-temperature regime where the exchange coupling is enhanced.

Therefore we investigate the low-temperature transport behavior of a heterostructure of the 3D TI Bi_2Se_3 and a [Co/Pt] multilayer, a metallic FM with perpendicular magnetic anisotropy. Magnetoresistance (MR) is measured as a function of an external magnetic field along different orientations and temperatures. We observe in these devices spin-valve-like MR responses with 20% abrupt change in resistance between bistable MR states. The spin-valve-like MR shows magnetic hysteresis and appears below 1 K for field sweeps along in-plane and out-of-plane directions. The MR switching field shows threefold symmetry with field sweep angle relative to the current direction, which may be associated with the symmetry of the crystal and the spin texture of the surface state. After comparing the spin-valve-like MR

to the MR of a control [Co/Pt] device, we suggest that the spin-valve-like MR originates from the interaction between the proximity-induced surface magnetism and the FM layer magnetization. Our results imply that at low temperatures, the proximity-induced magnetization can have a significant effect on the observed MR by altering the TI surface state, even at the interface of metallic FM and TI.

II. EXPERIMENT AND RESULTS

Our devices consist of Bi_2Se_3 flakes with Co/Pt multilayer (Pt(5 nm)/[Co(0.3)/Pt(1)]₈; [Co/Pt]) deposited on top, as depicted in Fig. 1(a) (see Methods). The Bi_2Se_3 is mechanically exfoliated onto Si/SiO₂ substrates. Flake thicknesses were characterized with atomic force microscopy and ranged between 20 and 30 nm. The longitudinal resistance of the devices were measured as a function of external magnetic field at various orientations and for temperatures lower than 1.5 K. Three devices on a substrate were measured for this study.

Co/Pt multilayer is chosen as our ferromagnetic layer for its well-studied magnetic properties and perpendicular magnetic anisotropy [31–33]. The perpendicular magnetic anisotropy of the FM layer is crucial, as the TI surface state is gapped only when the induced magnetization is directed normal to the surface. We characterized magnetic properties of [Co/Pt] films patterned into Hall bars independent from the TI/FM devices. Figure 1(b) shows the anomalous Hall effect (AHE) of the sputtered [Co/Pt] film at 300 K and 100 mK, which confirms the perpendicular magnetic anisotropy at these temperatures and shows the magnetization switching at perpendicular fields above 50 mT. The [Co/Pt] Hall bar also exhibits typical $\cos^2(\theta)$ anisotropic MR for metallic FM systems [34] for a 1-T external field \mathbf{H} rotated in the zx plane. Figure 1(c) shows anisotropic MR taken at $T = 300$ K and 100 mK, with anisotropic MR amplitude as large as 0.2% at 100 mK.

Unlike the [Co/Pt] control films which exhibit conventional ferromagnetic anisotropic MR, our Bi_2Se_3 /[Co/Pt] devices exhibit spin-valve-like hysteretic MR switching at temperatures below 1 K. In particular, for the device made with a 26-nm Bi_2Se_3 flake, the MR signal for \mathbf{H} sweeps along the current direction (x) at $T = 100$ mK [Fig. 2(a)] and shows sharp switching between low (R_{low}) and high (R_{high}) resistance states at $H_x \sim \pm 5$ mT, an approximately 20% change in MR. \mathbf{H} sweeps along the y direction [H_y sweep; Fig. 2(b)], resulting in an almost identical MR curve as H_x sweeps, only slightly differing in the switching field value. The out-of-plane field sweeps [Fig. 2(c)] also show switching with a 20% MR change, although with switching field values (from R_{low} to R_{high}) closer to 0 mT. As the temperature is raised, both the R_{high} and the coercivity of the MR hysteresis gradually decrease for in-plane and out-of-plane sweeps [Figs. 3(a) and 3(b)], eventually disappearing above 1.3 K.

From our separate measurement of Bi_2Se_3 and [Co/Pt] control samples, the sheet resistance of each layer is estimated to be $3.6 \text{ k}\Omega/\text{sq}$ and $36.3 \text{ }\Omega/\text{sq}$, respectively. The precise estimation of the magnitude of the effect is difficult; because of the device design and the resistance at the TI-FM interface, the apparent magnitude could be a significant underestimation considering the parallel conduction.

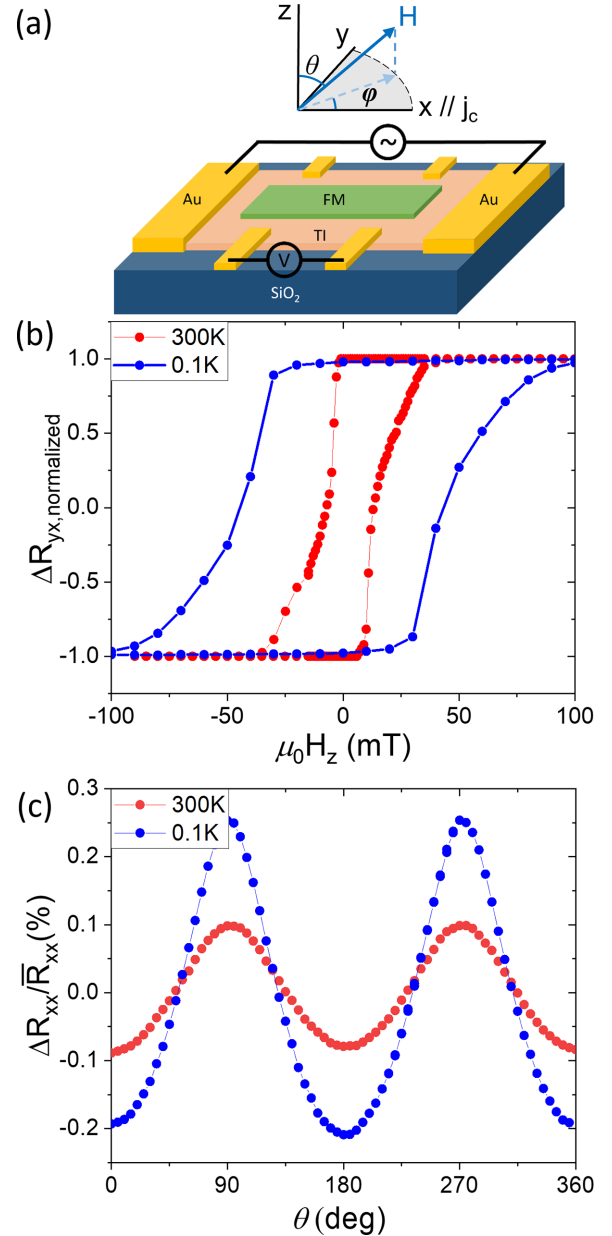


FIG. 1. (a) Schematic of a Bi_2Se_3 /[Co/Pt] device. x , y , z , ϕ , and θ are defined as shown. Typical (b) AHE and (c) anisotropic MR in [Co/Pt] Hall bar structure, measured at $T = 100$ mK and 300 K. Anisotropic MR was measured with 1-T field rotated out of plane in the zx plane as shown in the schematic. AHE result demonstrates Co/Pt magnetization switching at $H_z \sim 50$ mT at 100 mK.

The observed MR behavior in our device resembles that of a spin valve. Typical spin-valve systems consist of two FM layers separated by a thin nonmagnetic layer. Giant magnetoresistance (GMR) [35,36] describes the resistance difference depending on the relative orientations of the magnetizations caused by spin-dependent electron scattering in the spin valves; the system is in a low(high) resistance state when the magnetizations of the FM layers are parallel (antiparallel). The GMR switching in spin valves corresponds to the magnetization switching in a layer.

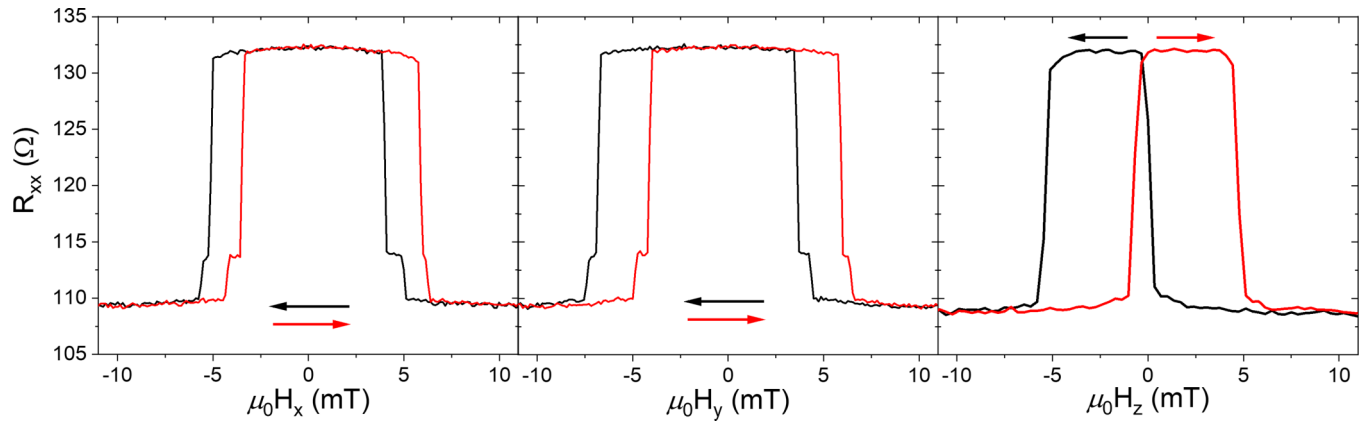


FIG. 2. Spin-valve-like hysteretic MR response of TI/[Co/Pt] device at $T = 100$ mK for magnetic field sweeps (a) along the current (x), (b) perpendicular to the current (y), and (c) out of plane (z). In all cases, the abrupt 20% MR change between high- and low-resistance states happens at low fields $H < 8$ mT, much lower than the switching field of the [Co/Pt] FM layer.

Although the spin-valve-like MR switching in our TI/FM devices is similar to GMR switching in its shape and magnitude, it cannot be fully explained with conventional GMR-like switching. In particular, our observation of MR switching for both in-plane and out-of-plane field sweeps is uncommon among conventional spin valves. More importantly, the heterostructure consists of only one magnetic layer and lacks a second layer of FM necessary to form a spin valve. We instead believe our results are consistent with the proximity-induced magnetization on the TI surface creating a spin-valve structure along with the top [Co/Pt] layer. The possible origins of the MR switching will be discussed in more detail below.

To clarify the origins of the MR switching, we performed measurements where the field is swept along an in-plane angle ϕ between the field and the current. Figure 4(a) reveals that the spin-valve-like MR behavior and bistable MR states appear independently of in-plane field angle ϕ , as illustrated in Fig. 1(a). Surprisingly, the MR switching fields for low-to-high (H_{LtoH}) and high-to-low (H_{HtoL}) resistance states have periodicity with ϕ as featured in Fig. 4(b). Polar plots of R vs

H_ϕ in Figs. 4(c) and 4(d) also show the correlation between the switching fields and ϕ ; both H_{LtoH} and H_{HtoL} have maximum values for $\phi = -60, 60, \text{ and } 180^\circ$, setting the trend for the apparent threefold symmetry of H_{LtoH} and H_{HtoL} . This threefold symmetry is not expected for conventional GMR.

III. DISCUSSION

As the electric current flows through both Bi_2Se_3 and [Co/Pt], the MR of the bilayer device may include MR from the metallic FM layer. Through comparison to [Co/Pt] MR [Figs. 1(b) and 1(c)], we determine that multiple features of the Bi_2Se_3 /[Co/Pt] spin-valve-like MR are inconsistent with the ferromagnetic MR of the [Co/Pt] layer alone and suggest the spin-valve-like MR switching of the heterostructure likely originates from the proximity-magnetized surface state.

The first discrepancy is the difference between the magnetization switching characteristics of the bilayer devices and that of the [Co/Pt]. Low-temperature [Co/Pt] magnetometry and AHE measurements show MR switching at

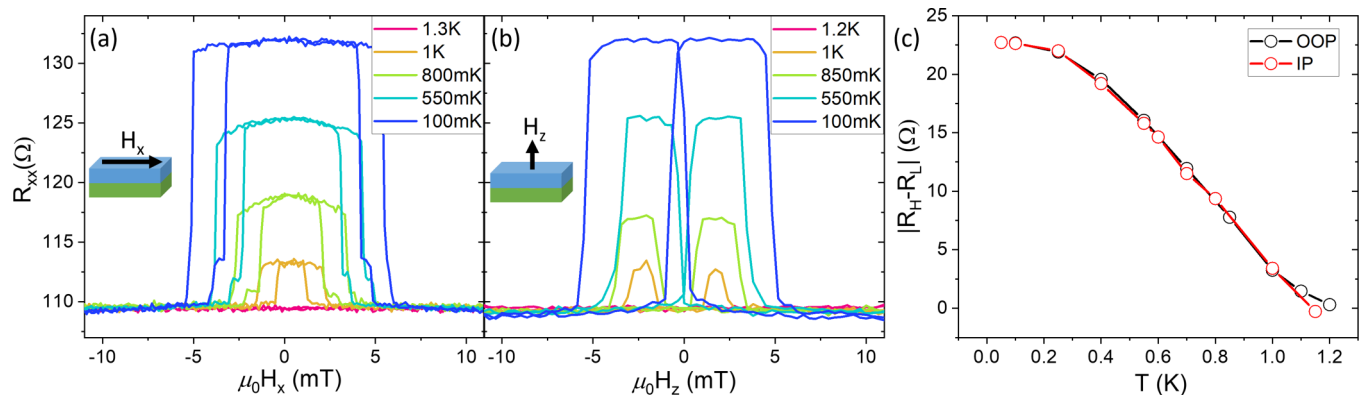


FIG. 3. Temperature dependence of the spin-valve-like MR response to (a) in-plane and (b) out-of-plane field sweeps. Both the high-MR state and the width of the hysteresis out of plane decrease as a function of increasing temperature, before the effect disappears after $T \sim 1$ K. (c) MR% plotted as a function of temperature. High- and low-MR states are considered identical for in-plane and out-of-plane field sweeps due to their same resistance at a given temperature.

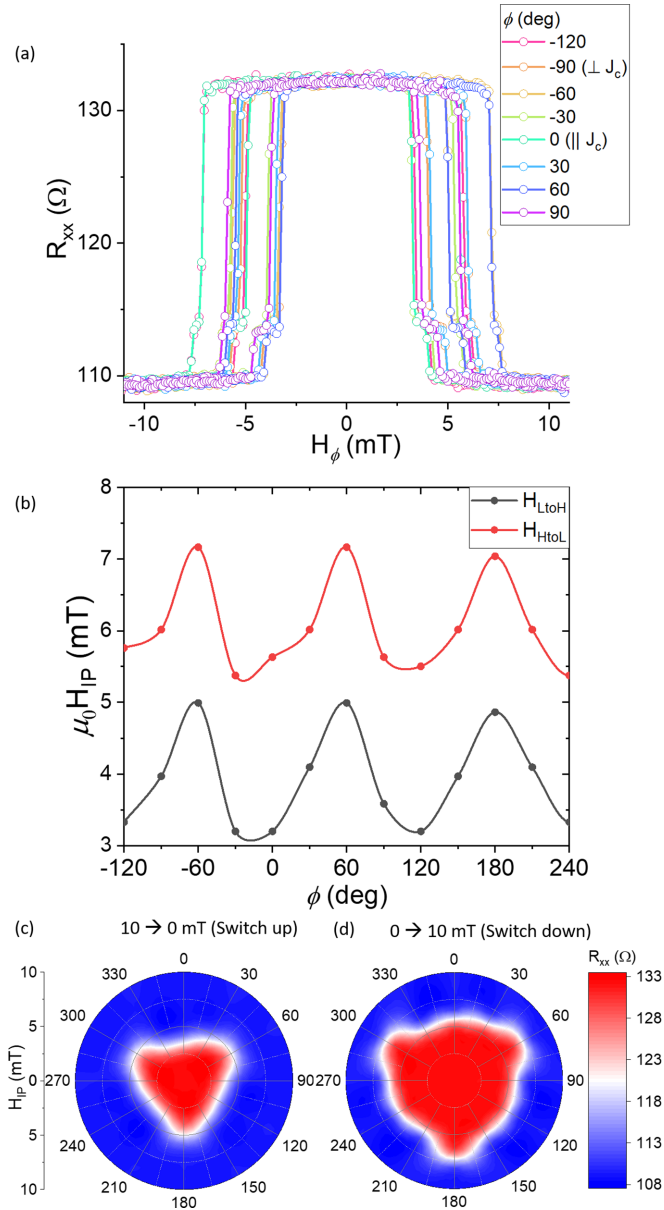


FIG. 4. (a) MR for in-plane field sweep measurements at different angles ϕ stepped by 30° . While the MR magnitude is constant, a threefold variation in H_{LtoH} and H_{HtoL} is evident. (b) H_{LtoH} and H_{HtoL} switching fields as a function of ϕ . The polar plots for (b) 10 \rightarrow 0 mT (switch up) and (c) 0 \rightarrow 10 mT (switch down) reveal threefold symmetry of the maximum switching fields that matches with the crystalline symmetry of Bi_2Se_3 , hence signaling the direct correlation of the spin-valve-like MR response and Bi_2Se_3 . The intermediate angles are interpolated.

$H_z \sim 50$ mT, whereas both H_{LtoH} and H_{HtoL} are less than 10 mT. The magnetization direction of the top FM layer is thus mostly unchanged and oriented along $\pm z$ direction near these field values. Also, unlike the FM film that has evident perpendicular magnetic anisotropy, the bilayer devices exhibit two MR states for both in-plane and out-of-plane field sweeps. As seen in the in-plane field sweep of the [Co/Pt] film, anisotropic MR smoothly changes from high resistance to low resistance as the magnetization of the FM layer is

rotated along the field direction. This can be contrasted with the abrupt switching with the in-plane field evident in the bilayer devices, suggesting the anisotropy of the system does not match the perpendicular magnetic anisotropy of the FM layer.

Secondly, the spin-valve-like MR emerges only below 1 K in the bilayer. In contrast, apart from the increased anisotropic MR signal at low temperatures that can be explained as the increase in the saturation magnetization, the MR of the [Co/Pt] at 0.1 mK and 300 K shows no qualitative difference, as expected. Given that both the magnitude and the width of the hysteresis of the spin-valve-like MR in the bilayer devices have dramatic temperature dependence, the spin-valve-like MR cannot be attributed to the FM layer.

Finally, the magnitude of the bilayer MR does not match that of the anisotropic MR from the [Co/Pt] film. At 0.1 K, the most dominant MR from [Co/Pt] is anisotropic MR, which peaks at around 0.2% of the normal resistance—a typical magnitude of anisotropic MR in ferromagnetic metals. On the other hand, the spin-valve-like MR in the bilayer device reaches up to 20% change in resistance, which can be explained solely by the anisotropic MR from FM.

All of the differences in MR of the [Co/Pt] and the bilayer device confirm that the FM layer is not the direct source of the MR. Because the Bi_2Se_3 alone is not magnetic, the MR switching is consistent with a weak magnetic ordering at the TI-FM interface, induced via exchange coupling to the top FM layer. Further, the data is consistent with previous results showing that FM insulators are directly coupled to TI surface states. In particular, $\text{Bi}_2\text{Se}_3/\text{YIG}$ systems have exhibited large MR that decrease in both amplitude [20,25] and coercivity [25] as the temperature is cooled down below the critical temperature. Similar to our $\text{Bi}_2\text{Se}_3/[\text{Co}/\text{Pt}]$ devices, $\text{Bi}_2\text{Se}_3/\text{YIG}$ systems also exhibit hysteretic MR switching for both in-plane and out-of-plane field sweeps [20]. These results were attributed to the proximity-magnetized TI surface, with the exchange gap closing and opening with an applied external magnetic field.

The threefold symmetry of the switching fields (H_{LtoH} and H_{HtoL}) can be related to the crystal structure of Bi_2Se_3 , which has a C_3 symmetry in the ab plane. Rhombohedral crystal structure along with large spin-orbit coupling in Bi_2Se_3 causes the spin texture of the spin-momentum locked surface states to have a C_3 symmetric higher-order perturbation referred to as hexagonal warping [37]. Although the band hybridization annihilates the Dirac surface states, first-principle studies of the hybridization of Dirac surface state in TI and metallic FM layers demonstrated that the descendent interface states would inherit the spin texture of the topological surface states and be localized at the surface [29]. Furthermore, multiple theories and experiments [16,20,25,38,39] have shown that the magnetic anisotropy of the proximity-induced magnetization in the TI surface does not necessarily follow that of the ferromagnet providing the exchange coupling. Given the above understanding, the threefold symmetry in the MR switching fields likely originate from the TI. We believe that this is the first observation of threefold-symmetric MR switching behavior in proximity-magnetized TI systems.

As mentioned earlier, the magnitude and the shape of the MR effect is most similar to that of GMR observed in

spin-valve systems. Based on this and our observations, we suggest a simple phenomenological model that can qualitatively explain the MR effect: At zero field, the proximity-induced magnetic order in the TI surface has a very weak anisotropy along the out-of-plane direction, antiparallel to the magnetization of the FM layer. This magnetic state in the TI is very sensitive to a small external field in both in-plane and out-of-plane directions. The spin-valve-like MR switching can then be interpreted as a GMR signal from a spin valve consisting of induced TI surface magnetization and the top [Co/Pt] layer.

Understanding the details of the magnetized TI states requires further studies. Many MR features previously measured in various TI/FMI systems [20–22,26] have been attributed to conduction channels through a domain wall. In this scheme, it is thought that domains in the TI surface whose magnetization is oriented normal to the surface have gapped surface states associated with the high resistance. Domain walls formed during the switching process have magnetization in the in-plane direction, so gapless surface states can be preserved. The conduction channels along these domain walls lead to the low-resistance states, causing the MR to drop at the magnetization switching fields. However, spin-valve-like MR switching observed in our TI/FM devices does not coincide with the magnetization switching of the top FM layer, nor does the TI layer retain the topological surface state due to the hybridization.

The spin-valve-like MR may involve more complicated magnetization configurations. One possible explanation is the presence of unstable skyrmions. Skyrmion-like spin textures have been previously detected for TI/FM bilayer systems via measurements of topological Hall effect [40,41] and scanning transmission x-ray microscopy [42]. When a skyrmion is present at the TI/FM interface, the perpendicular moment at its core will give rise to the high-resistance state near zero field. The external field of a few mT can destroy the skyrmion in a confined geometry [43], resulting in the MR switching into a low-resistance state. A further systematic study involving the detection of the interfacial skyrmions would be required to confirm this.

We would like to note that two other devices with different Bi₂Se₃ thicknesses exhibited large MR switching of varying magnitudes (see Supplemental Material S3 [44]). In Bi₂Se₃/EuS bilayer, neutron scattering revealed 2 nm of the TI surface is proximity magnetized at 5 K [28]. However, the bulk states of the TI can contribute to the transport for Bi₂Se₃ thicker than six quintuple layers [2]. A systematic thickness-dependent examination would illuminate the role of the bulk and the surface states and help clarify the origin of the MR effect.

IV. CONCLUSION

In summary, Bi₂Se₃/[Co/Pt] devices exhibited spin-valve-like hysteretic MR for in-plane and out-of-plane field sweeps at temperatures below 1 K. The MR's temperature dependence, anisotropy, and in-plane angle dependence indicate that it is likely associated with the proximity-induced magnetic ordering at the TI surface rather than the FM layer. The threefold symmetry of the switching fields, which may be related to the crystal symmetry of the Bi₂Se₃, also support its interfacial origin. We speculate that the FM layer and the surface magnetization of the Bi₂Se₃ creates a spin valve and the observed MR is a GMR-like effect. Our experimental result indicates that even in heterostructures of TI and metallic FM, the proximity-induced surface magnetization can have a sizable effect on the MR behavior, emphasizing the importance of proximity magnetization in topological spintronics research.

V. METHODS

Bi₂Se₃ TI crystal was mechanically exfoliated on a diced Si/SiO₂(300 nm) wafer using the conventional tape method. Each Bi₂Se₃ flake was characterized with atomic force microscopy to be 20–40 nm in thickness and order of a few micrometers laterally. Pt(5nm)/[Co(0.3)/Pt(1)]₈/Pt(1) FM layer was deposited using a sputter system built in-house. Electron-beam lithography was used to pattern the top FM layer and the electrical contacts. Ti(5)/Au(50) was deposited with an electron-beam evaporator to create contacts.

Magnetometry of the film was done using Quantum Design (QD) MPMS3 vibrating sample magnetometer. All transport measurements were performed using SR830 lock-in amplifiers. Anisotropic MR and AHE measurement of patterned [Co/Pt] at room temperature was done in QD PPMS Dynacool instruments. Low-temperature measurements were performed in an Oxford Triton 200 dilution refrigerator system equipped with 6-1-1 vector superconducting magnets.

ACKNOWLEDGMENTS

This work is supported by the Army Research Office for measurements and analysis under W911NF2010024 and by the National Science Foundation for sample fabrication under the University of Illinois at Urbana Champaign, Materials Research Science and Engineering Center Grant No. DMR-1720633. Research performed using the QD MPMS3 and PPMS instruments was carried out in part in the Materials Research Laboratory Central Research Facilities, University of Illinois.

-
- [1] L. Fu, C. L. Kane, and E. J. Mele, Topological insulators in three dimensions, *Phys. Rev. Lett.* **98**, 106803 (2007).
- [2] H. Zhang, C.-X. Liu, X.-L. Qi, X. Dai, Z. Fang, and S.-C. Zhang, Topological insulators in Bi₂Se₃, Bi₂Te₃, and Sb₂Te₃ with a single Dirac cone on the surface, *Nat. Phys.* **5**, 438 (2009).

- [3] Y. Chen, J. G. Analytis, J.-H. Chu, Z. Liu, S.-K. Mo, X.-L. Qi, H. Zhang, D. Lu, X. Dai, Z. Fang *et al.*, Experimental realization of a three-dimensional topological insulator, Bi₂Te₃, *Science* **325**, 178 (2009).
- [4] E. Rongione, L. Baringthon, D. She, G. Patriarche, R. Lebrun, A. Lemaître, M. Morassi, N. Reyren, M. Mićica, J. Mangeney *et al.*, Spin-momentum locking and ultrafast spin-charge

- conversion in ultrathin epitaxial $\text{Bi}_{1-x}\text{Sb}_x$ topological insulator, *Adv. Sci.* **10**, 2301124 (2023).
- [5] C.-Z. Chang, J. Zhang, X. Feng, J. Shen, Z. Zhang, M. Guo, K. Li, Y. Ou, P. Wei, L.-L. Wang *et al.*, Experimental observation of the quantum anomalous Hall effect in a magnetic topological insulator, *Science* **340**, 167 (2013).
- [6] C.-Z. Chang, W. Zhao, D. Y. Kim, H. Zhang, B. A. Assaf, D. Heiman, S.-C. Zhang, C. Liu, M. H. Chan, and J. S. Moodera, High-precision realization of robust quantum anomalous Hall state in a hard ferromagnetic topological insulator, *Nat. Mater.* **14**, 473 (2015).
- [7] Y. Tokura, K. Yasuda, and A. Tsukazaki, Magnetic topological insulators, *Nat. Rev. Phys.* **1**, 126 (2019).
- [8] Y. Deng, Y. Yu, M. Z. Shi, Z. Guo, Z. Xu, J. Wang, X. H. Chen, and Y. Zhang, Quantum anomalous Hall effect in intrinsic magnetic topological insulator MnBi_2Te_4 , *Science* **367**, 895 (2020).
- [9] Y. Gong, J. Guo, J. Li, K. Zhu, M. Liao, X. Liu, Q. Zhang, L. Gu, L. Tang, X. Feng *et al.*, Experimental realization of an intrinsic magnetic topological insulator, *Chin. Phys. Lett.* **36**, 076801 (2019).
- [10] Y. Wang, D. Zhu, Y. Wu, Y. Yang, J. Yu, R. Ramaswamy, R. Mishra, S. Shi, M. Elyasi, K.-L. Teo *et al.*, Room temperature magnetization switching in topological insulator-ferromagnet heterostructures by spin-orbit torques, *Nat. Commun.* **8**, 1364 (2017).
- [11] J. Han, A. Richardella, S. A. Siddiqui, J. Finley, N. Samarth, and L. Liu, Room-temperature spin-orbit torque switching induced by a topological insulator, *Phys. Rev. Lett.* **119**, 077702 (2017).
- [12] M. Mogi, K. Yasuda, R. Fujimura, R. Yoshimi, N. Ogawa, A. Tsukazaki, M. Kawamura, K. S. Takahashi, M. Kawasaki, and Y. Tokura, Current-induced switching of proximity-induced ferromagnetic surface states in a topological insulator, *Nat. Commun.* **12**, 1404 (2021).
- [13] A. Mellnik, J. Lee, A. Richardella, J. Grab, P. Mintun, M. H. Fischer, A. Vaezi, A. Manchon, E.-A. Kim, N. Samarth *et al.*, Spin-transfer torque generated by a topological insulator, *Nature (London)* **511**, 449 (2014).
- [14] H. Wang, J. Kally, J. S. Lee, T. Liu, H. Chang, D. R. Hickey, K. A. Mkhoyan, M. Wu, A. Richardella, and N. Samarth, Surface-state-dominated spin-charge current conversion in topological-insulator-ferromagnetic-insulator heterostructures, *Phys. Rev. Lett.* **117**, 076601 (2016).
- [15] M. Jamali, J. S. Lee, J. S. Jeong, F. Mahfouzi, Y. Lv, Z. Zhao, B. K. Nikolic, K. A. Mkhoyan, N. Samarth, and J.-P. Wang, Giant spin pumping and inverse spin Hall effect in the presence of surface and bulk spin-orbit coupling of topological insulator Bi_2Se_3 , *Nano Lett.* **15**, 7126 (2015).
- [16] M. Li, C.-Z. Chang, B. J. Kirby, M. E. Jamer, W. Cui, L. Wu, P. Wei, Y. Zhu, D. Heiman, J. Li *et al.*, Proximity-driven enhanced magnetic order at ferromagnetic-insulator-magnetic-topological-insulator interface, *Phys. Rev. Lett.* **115**, 087201 (2015).
- [17] J. Liu and T. Hesjedal, Magnetic topological insulator heterostructures: A review, *Adv. Mater.* **35**, 2102427 (2023).
- [18] S. V. Eremeev, V. N. Men'shov, V. V. Tugushev, P. M. Echenique, and E. V. Chulkov, Magnetic proximity effect at the three-dimensional topological insulator/magnetic insulator interface, *Phys. Rev. B* **88**, 144430 (2013).
- [19] V. N. Men'shov, V. V. Tugushev, S. V. Eremeev, P. M. Echenique, and E. V. Chulkov, Magnetic proximity effect in the three-dimensional topological insulator/ferromagnetic insulator heterostructure, *Phys. Rev. B* **88**, 224401 (2013).
- [20] M. Lang, M. Montazeri, M. C. Onbasli, X. Kou, Y. Fan, P. Upadhyaya, K. Yao, F. Liu, Y. Jiang, W. Jiang *et al.*, Proximity induced high-temperature magnetic order in topological insulator-ferrimagnetic insulator heterostructure, *Nano Lett.* **14**, 3459 (2014).
- [21] P. Wei, F. Katmis, B. A. Assaf, H. Steinberg, P. Jarillo-Herrero, D. Heiman, and J. S. Moodera, Exchange-coupling-induced symmetry breaking in topological insulators, *Phys. Rev. Lett.* **110**, 186807 (2013).
- [22] C. Tang, C.-Z. Chang, G. Zhao, Y. Liu, Z. Jiang, C.-X. Liu, M. R. McCartney, D. J. Smith, T. Chen, J. S. Moodera *et al.*, Above 400-K robust perpendicular ferromagnetic phase in a topological insulator, *Sci. Adv.* **3**, e1700307 (2017).
- [23] R. Watanabe, R. Yoshimi, M. Kawamura, M. Mogi, A. Tsukazaki, X. Yu, K. Nakajima, K. S. Takahashi, M. Kawasaki, and Y. Tokura, Quantum anomalous Hall effect driven by magnetic proximity coupling in all-telluride based heterostructure, *Appl. Phys. Lett.* **115**, 102403 (2019).
- [24] C.-Y. Yang, L. Pan, A. J. Grutter, H. Wang, X. Che, Q. L. He, Y. Wu, D. A. Gilbert, P. Shafer, E. Arenholz *et al.*, Termination switching of antiferromagnetic proximity effect in topological insulator, *Sci. Adv.* **6**, eaaz8463 (2020).
- [25] J. Sklenar, Y. Zhang, M. B. Jungfleisch, Y. Kim, Y. Xiao, G. J. MacDougall, M. J. Gilbert, A. Hoffmann, P. Schiffer, and N. Mason, Proximity-induced anisotropic magnetoresistance in magnetized topological insulators, *Appl. Phys. Lett.* **118**, 232402 (2021).
- [26] V. Gupta, R. Jain, Y. Ren, X. S. Zhang, H. F. Alnaser, A. Vashist, V. V. Deshpande, D. A. Muller, D. Xiao, T. D. Sparks *et al.*, Gate-tunable anomalous Hall effect in a 3D topological insulator/2D magnet van der Waals heterostructure, *Nano Lett.* **22**, 7166 (2022).
- [27] J. S. Lee, A. Richardella, R. D. Fraleigh, C.-x. Liu, W. Zhao, and N. Samarth, Engineering the breaking of time-reversal symmetry in gate-tunable hybrid ferromagnet/topological insulator heterostructures, *npj Quantum Mater.* **3**, 51 (2018).
- [28] F. Katmis, V. Lauter, F. S. Nogueira, B. A. Assaf, M. E. Jamer, P. Wei, B. Satpati, J. W. Freeland, I. Eremin, D. Heiman *et al.*, A high-temperature ferromagnetic topological insulating phase by proximity coupling, *Nature (London)* **533**, 513 (2016).
- [29] Y.-T. Hsu, K. Park, and E.-A. Kim, Hybridization-induced interface states in a topological-insulator-ferromagnetic-metal heterostructure, *Phys. Rev. B* **96**, 235433 (2017).
- [30] G. J. De Coster and M. J. Gilbert, Essential design criteria for topological electronics and spintronics, in *2021 IEEE International Electron Devices Meeting (IEDM)* (IEEE, New York, 2021), pp. 38.3.1–38.3.4.
- [31] D. Weller, L. Folks, M. Best, E. E. Fullerton, B. Terris, G. Kusinski, K. Krishnan, and G. Thomas, Growth, structural, and magnetic properties of high coercivity Co/Pt multilayers, *J. Appl. Phys.* **89**, 7525 (2001).
- [32] S. Maat, K. Takano, S. S. P. Parkin, and E. E. Fullerton, Perpendicular exchange bias of Co/Pt multilayers, *Phys. Rev. Lett.* **87**, 087202 (2001).

- [33] J. Oh, L. Humbard, V. Humbert, J. Sklenar, and N. Mason, Angular evolution of thickness-related unidirectional magnetoresistance in Co/Pt multilayers, *AIP Adv.* **9**, 045016 (2019).
- [34] T. McGuire and R. Potter, Anisotropic magnetoresistance in ferromagnetic 3D alloys, *IEEE Trans. Magn.* **11**, 1018 (1975).
- [35] M. N. Baibich, J. M. Broto, A. Fert, F. N. Van Dau, F. Petroff, P. Etienne, G. Creuzet, A. Friederich, and J. Chazelas, Giant magnetoresistance of (001) Fe/(001) Cr magnetic superlattices, *Phys. Rev. Lett.* **61**, 2472 (1988).
- [36] G. Binasch, P. Grünberg, F. Saurenbach, and W. Zinn, Enhanced magnetoresistance in layered magnetic structures with antiferromagnetic interlayer exchange, *Phys. Rev. B* **39**, 4828 (1989).
- [37] L. Fu, Hexagonal warping effects in the surface states of the topological insulator Bi_2Te_3 , *Phys. Rev. Lett.* **103**, 266801 (2009).
- [38] Y. G. Semenov, X. Duan, and K. W. Kim, Electrically controlled magnetization in ferromagnet-topological insulator heterostructures, *Phys. Rev. B* **86**, 161406(R) (2012).
- [39] S.-Y. Xu, M. Neupane, C. Liu, D. Zhang, A. Richardella, L. Andrew Wray, N. Alidoust, M. Leandersson, T. Balasubramanian, J. Sánchez-Barriga *et al.*, Hedgehog spin texture and Berry's phase tuning in a magnetic topological insulator, *Nat. Phys.* **8**, 616 (2012).
- [40] K. Yasuda, R. Wakatsuki, T. Morimoto, R. Yoshimi, A. Tsukazaki, K. Takahashi, M. Ezawa, M. Kawasaki, N. Nagaosa, and Y. Tokura, Geometric Hall effects in topological insulator heterostructures, *Nat. Phys.* **12**, 555 (2016).
- [41] J. Chen, L. Wang, M. Zhang, L. Zhou, R. Zhang, L. Jin, X. Wang, H. Qin, Y. Qiu, J. Mei *et al.*, Evidence for magnetic skyrmions at the interface of ferromagnet/topological-insulator heterostructures, *Nano Lett.* **19**, 6144 (2019).
- [42] H. Wu, F. Groß, B. Dai, D. Lujan, S. A. Razavi, P. Zhang, Y. Liu, K. Sobotkewich, J. Förster, M. Weigand *et al.*, Ferrimagnetic skyrmions in topological insulator/ferrimagnet heterostructures, *Adv. Mater.* **32**, 2003380 (2020).
- [43] R. Juge, S.-G. Je, D. de Souza Chaves, S. Pizzini, L. D. Buda-Prejbeanu, L. Aballe, M. Foerster, A. Locatelli, T. O. Mentes, A. Sala *et al.*, Magnetic skyrmions in confined geometries: Effect of the magnetic field and the disorder, *J. Magn. Magn. Mater.* **455**, 3 (2018).
- [44] See Supplemental Material at <http://link.aps.org/supplemental/10.1103/PhysRevMaterials.8.054202> for 0.8 T linear field sweep data of the Bi_2Se_3 /[Co/Pt] device, linear field sweep data for a [Co/Pt] control device, large square switching MR from other Bi_2Se_3 /[Co/Pt] devices, repeatability of the MR switching, and anomalous Hall signal from a [Co/Pt] placed on top of 8 nm Bi_2Se_3 film grown via molecular beam epitaxy.